Part I
Biochemistry and Biophysics

1
Investigations on Fluorine-Labeled Ribonucleic Acids by ^{19}F NMR Spectroscopy

Christoph Kreutz and Ronald Micura

1.1
Introduction

1.1.1
NMR Spectroscopic Properties of the ^{19}F Nucleus

1.1.1.1 General NMR Spectroscopic Properties

Fluorine, with its unique nuclear magnetic resonance (NMR) spectroscopic parameters, has 100% natural abundance, possesses an intrinsic NMR sensitivity almost as high as protons (83%), and offers a chemical shift dispersion that is about 100-fold that of protons (Table 1.1). These properties make fluorine an ideal candidate to be used as an alternative spin label complementary to ^{13}C- and ^{15}N-labeling. Thus, the introduction of fluorine produces a strong NMR signal that appears against a background devoid of signals from other nuclei.

Table 1.1 Gyromagnetic ratios (γ), NMR frequencies (ν) in a 9.4 T magnetic field, and natural abundances (a) of selected nuclides.

Nucleus	γ [rad.T^{-1} s^{-1} 10^7]	ν [MHz]	a [%]
^{1}H	26.75	400.0	99.985
^{13}C	6.73	100.6	1.108
^{15}N	–2.71	40.5	0.37
^{19}F	25.18	376.5	100.0
^{31}P	10.84	162.1	100.0

1.1.1.2 ^{19}F versus ^{1}H NMR Spectroscopy

A biopolymer exhibits a NMR spectrum, which is composed of the typical resonance frequencies (chemical shifts) of the different building units that comprise the

Modified Nucleosides: in Biochemistry, Biotechnology and Medicine. Edited by Piet Herdewijn

ISBN: 978-3-527-31820-9

biomolecule. In ^{1}H NMR spectroscopy, chemical shift values typically span a range of approximately 10 to 15 ppm. This leads to severe overlap and resonance degeneracy in the proton NMR spectrum, in particular, in the case of large biomolecules or if other phenomena such as chemical exchange are present. For example, resonances of the imino protons (protons that participate in Watson–Crick base pairing) are well separated for the 32 nt DNA/RNA hybrid depicted in Figure 1.1, whereas the residual resonances from sugar and nucleobase moieties show severe overlap. Multidimensional NMR methods and labeling techniques (^{13}C and ^{15}N) are required to overcome this hurdle.

In contrast, fluorine chemical shifts span a very wide range due to the intrinsic electronic situation of the fluorine nucleus (on average the ^{19}F nucleus is surrounded by nine electrons, whereas the hydrogen nucleus is only surrounded by a single electron). Thus, the problem of resonance degeneracy in ^{19}F NMR spectroscopy is almost non-existent (Figure 1.2). Chemical shift values are listed in Table 1.2 for fluorinated organic groups relative to various reference compounds.

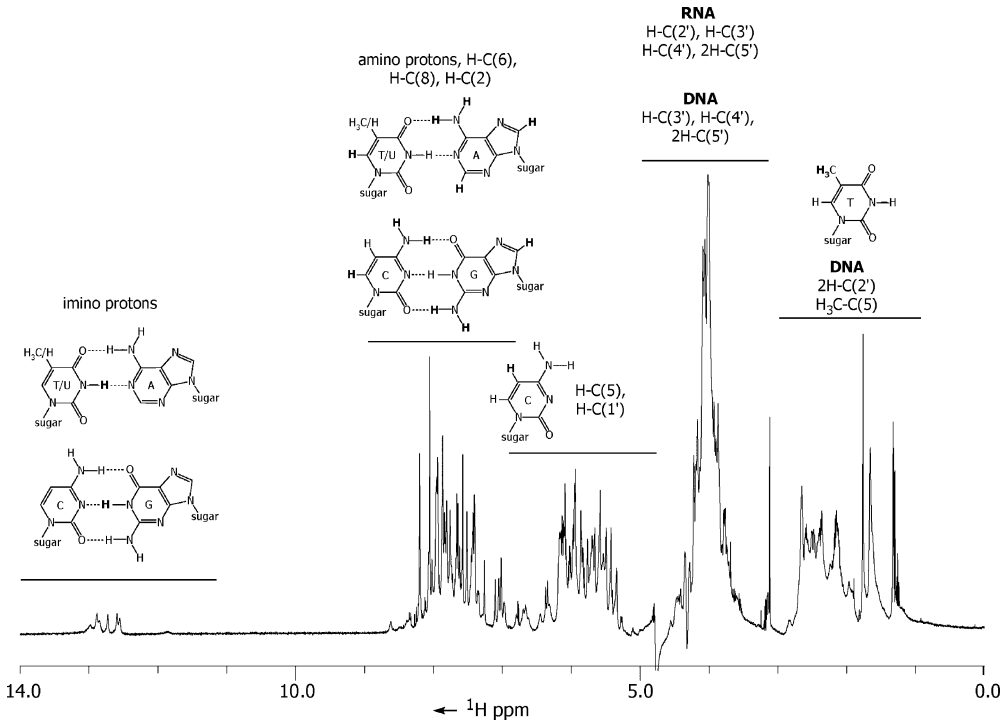

Figure 1.1 Typical one-dimensional proton NMR spectrum of a nucleic acid system (1.0 mM DNA/RNA hybrid, 50 mM sodium phosphate buffer, pH 7, 283 K, D_2O/H_2O ratio 1/9). Based on the local magnetic field induced by the chemical environment, resonances belonging to the different building units of the biopolymer (e.g., sugars, nucleobases) can be identified. However, with a chemical shift range of about 15 ppm, severe resonance overlap is encountered in the ^{1}H NMR spectrum.

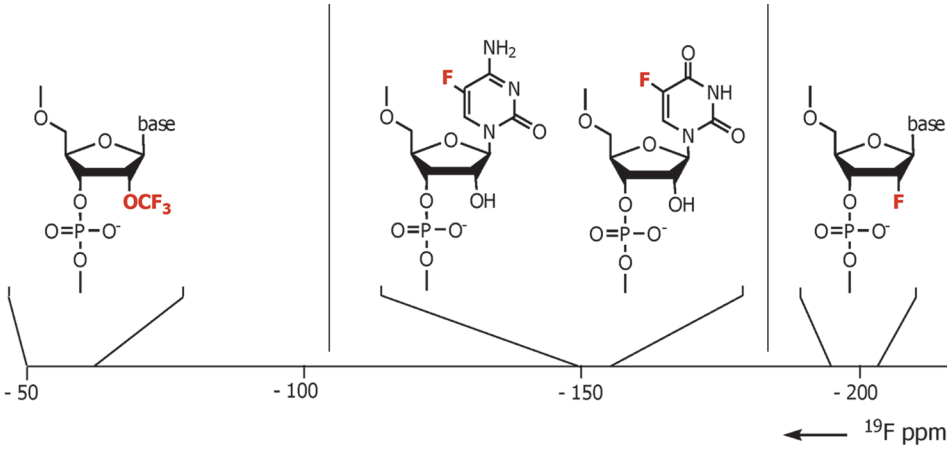

Figure 1.2 Typical chemical shift values that are found in fluorine-modified oligonucleotides (referenced to $CFCl_3$). With a chemical shift dispersion that is about 100-fold that of protons, resonance degeneracy is hardly encountered in ^{19}F NMR spectra.

1.1.1.3 Factors Affecting the ^{19}F Chemical Shift in Biomolecules

One of the most useful properties of the ^{19}F nucleus is the high sensitivity of the fluorine shielding parameter to changes in the local environment. This makes fluorine an ideal candidate for monitoring functional important transitions in biological systems via NMR spectroscopic methods. In the following, we will briefly describe two situations where changes in fluorine chemical shifts are expected: namely, the folding of a biomolecule; and the binding of a ligand at a receptor site.

Starting from a biomolecule containing a fluorinated reporter group in its native functional state, the fluorine spin label can be used to monitor transition to the denatured (unfolded) state. The local environment of the fluorine is supposed to be changed significantly by the unfolding process. In the unfolded state, the fluorine is exposed and thereby subjected to interactions that are predominantly due to solvent molecules. In contrast, during the folding process from an unfolded to the native state, secondary and tertiary structure elements are formed. Thus, the fluorine

Table 1.2 Chemical shift values of fluorinated functional groups.

Chemical group	Chemical shift relative to $CFCl_3$ [ppm]
$-C(F)H-$	−210
$-CF_2-$	−140
$R-C_6H_4-F$	−140
$-CF_2-C(O)-$	−125
$-CH-CF_3$	−75
$-C(O)-CF_3$	−81
$-SO_2F$	50

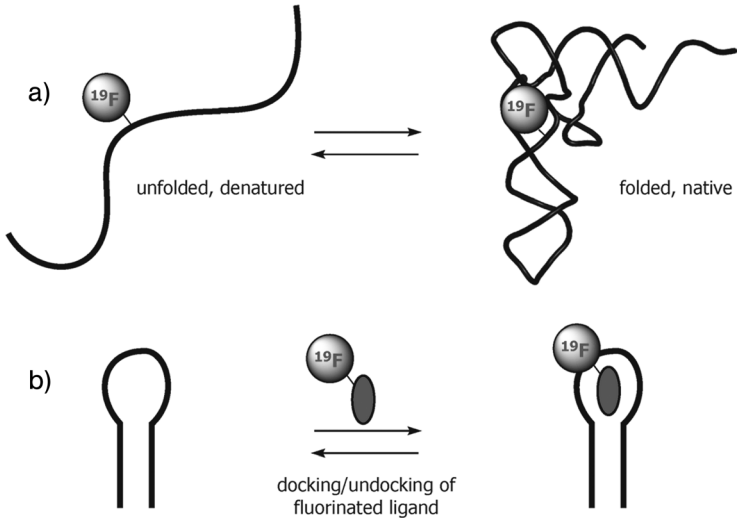

Figure 1.3 Functionally important transitions of biomolecules for ^{19}F NMR spectroscopic applications. (a) A ^{19}F spin label can be used to monitor the transition of a biomolecule from the unfolded to the folded, functional state. (b) Binding and release of a ligand at a receptor site can be detected by observing the ^{19}F resonance of the fluorinated ligand.

reporter nucleus becomes buried in the structural network made up by the biomolecule's architecture. Thereby, the chemical environment of the fluorine can be dramatically changed and interactions with solvent molecules are expected to be disrupted, resulting in a different chemical shift of the fluorine reporter (Figure 1.3a).

The second aspect of how ^{19}F NMR spectroscopy is involved in studies of biomolecules relates to interactions with a ligand. For a fluorinated small molecule that binds at a receptor site, the electric fields, short-range contacts and hydrogen-bonding possibilities experienced by the fluorine are different in the free versus receptor-bound states, and these will be reflected in a change of the chemical shift value (Figure 1.3b).

1.1.1.4 **Fluorine Relaxation in Biological Systems**

The fluorine spins relax mainly by two pathways. First, dipole–dipole interactions with the surrounding proton spins offer an effective relaxation pathway. Second, the anisotropy of the fluorine chemical shift leads to an enhanced relaxation rate.

Dipole–dipole interactions are very useful as they can lead to $^{19}F/^{19}F$ and $^{1}H/^{19}F$ nuclear Overhauser effects (NOEs) that provide interesting information about internuclear distances in the same way as do proton–proton NOEs. Fluorine relaxation can also provide a quantitative estimation of the degree of mobility in different parts of a large biomolecule. Furthermore, fluorine NMR experiments are also sensitive to the rates of processes which interchange the environments of the observed spins, and thus can produce quantitative data about the rates of processes, such as conformational change and ligand exchange. For a detailed discussion on fluorine relaxation, the reader is referred to the review by Gerig [1].

1.1.1.5 Solvent-Induced Isotope Shifts of ^{19}F NMR Resonances

Experiments have shown that a fluorine signal from a water-soluble molecule is deshielded by about 0.2 ppm when the solvent is changed from water (H_2O) to deuterium oxide (D_2O) [2, 3]. The magnitude of the effect thus reflects the extent to which a fluorine nucleus in a macromolecule is exposed to solvent. An established way of considering solvent exposure in fluorinated biomolecules is simply gradually to replace H_2O with D_2O, as an inverse correlation is found between the buriedness and the solvent-induced isotope shift (SIIS) effect [2]. The ^{19}F NMR resonances of the exposed regions of a biomacromolecule can be shifted by about 0.2 ppm by replacing H_2O with D_2O, whereas buried fluorinated residues do not experience any (or only a weak) SIIS. By replacing H_2O with D_2O, all exchangeable protons become replaced by deuterons; this leads to a slightly changed chemical environment, and may also bear influence on the ^{19}F H_2O/D_2O isotope shift. In other studies, $H_2{}^{18}O$ was used to induce an isotope shift of ^{19}F resonances of small fluorinated molecules and a 16 nt RNA containing a single 5-fluorouridine [4, 5].

1.1.2 ^{19}F NMR Spectroscopy of Proteins

1.1.2.1 Incorporation of Fluorinated Amino Acids into Proteins

A wide variety of synthetic methods are available for the preparation of fluorinated derivatives of most of the common amino acids. The placement of these fluorinated materials into proteins has been accomplished by different strategies, including chemical synthesis and biosynthetic incorporation by organisms. Today, some fluorine-bearing aromatic amino acids, such as 4-fluorophenylalanine, 4-trifluoromethylphenylalanine, 6- and 5-fluorotryptophan, and 3-fluorotyrosine, are commercially available (Figure 1.4).

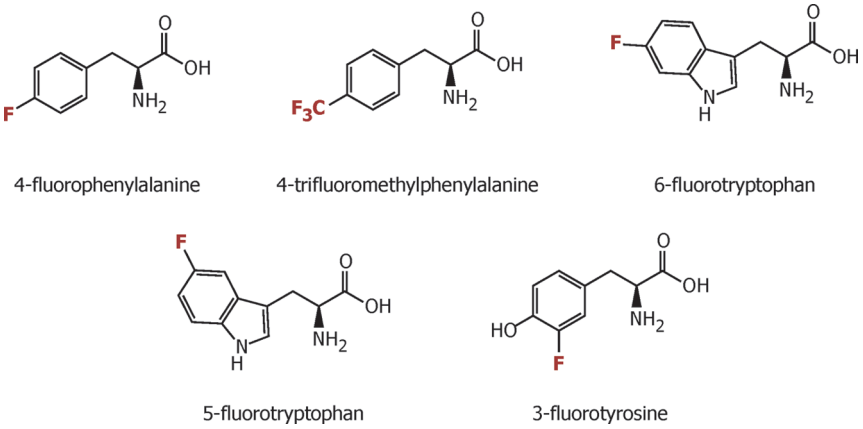

Figure 1.4 Fluorinated aromatic amino acids that can be incorporated into proteins by chemical or biosynthetic methods. In general, the fluorinated amino acids are well accepted in the native protein structure, where they serve as high-sensitivity spin labels for ^{19}F NMR spectroscopic applications.

By far the most widely used method for placing fluorinated amino acids into the primary sequence of proteins is biosynthesis of the protein by a living organism. Fluorinated bacterial proteins are usually obtained by using bacterial strains that are auxotrophic for tryptophan by adding fluorinated tryptophan to the growth medium. A variety of other approaches exist to incorporate aromatic fluorinated amino acids, including the use of glyphosphate or 3-β-indoleacrylic acid, both of which are inhibitors of aromatic amino acid synthesis [6, 7]. These biosynthetic approaches lead to the ubiquitous incorporation of fluorinated amino acids into the target protein, and the need to assign all observed ^{19}F resonances. If site-specific ^{19}F labeling of a protein is desired, then chemical synthesis of the peptide or protein is necessary. Alternative approaches to the site-specific incorporation of fluorinated aromatic amino acids by biosynthetic methods were also elaborated, for example by using an appropriately acylated suppressor tRNA that inserts the fluorinated amino acid in response to a stop codon substituted for the codon encoding the residue of interest [8]. In 1998, Furter *et al.* used such an approach to incorporate *p*-fluorophenylalanine in a site-directed manner into proteins [9]. The major advance here was the use of an *Escherichia coli* strain, which was equipped with a non-essential yeast aminoacyl-tRNA synthetase that charged its cognate yeast amber suppressor tRNA with the fluorinated amino acid analogue, which in turn was incorporated almost exclusively at a programmed stop codon. Although incorporation yields of up to 75% were obtained, the method also caused 3–7% of all phenylalanine residues to be replaced by the fluorinated counterpart.

Very recently, a further advance in site-specific labeling of proteins with ^{19}F modified amino acids was presented [10]. The site-specific introduction of trifluoromethyl-L-phenylalanine (tfm-Phe) was described by an orthogonal aminoacyl-tRNA synthetase/tRNA pair, capable of incorporating tfm-Phe into proteins. The synthetase/tRNA pair functions with high translational efficiency and fidelity for incorporating tfm-Phe using a nonsense codon in *E. coli*.

1.1.2.2 ^{19}F NMR Spectroscopic Studies of Proteins

Native and Denatured States of Green Fluorescent Protein Khan and coworkers successfully prepared uniformly 3-fluorotyrosine-labeled green fluorescent protein (GFP) [11], and subsequently assigned the observed ^{19}F resonances to all ten fluorotyrosines by successively replacing the fluorotyrosines by phenylalanines. Complete assignment was achieved with the additional aid of relaxation data and ^{19}F photochemically induced dynamic nuclear polarization (CIDNP). The ^{19}F resonances showed no overlaps, and were dispersed over a chemical shift range of 10 ppm. Most interestingly, two tyrosines (Tyr92 and Tyr143) exhibited a pair of signals that were interpreted by two ring-flip conformational states populated in the folded protein. The sensitivity enhancement by the photo-CIDNP mechanism revealed four ^{19}F tyrosine resonances which are solvent-exposed in the native state (Y39, Y151, Y182, and Y200).

Furthermore, the photo-CIDNP approach was used to characterize the denatured states of GFP. The photo-CIDNP spectra under unfolding conditions and using high

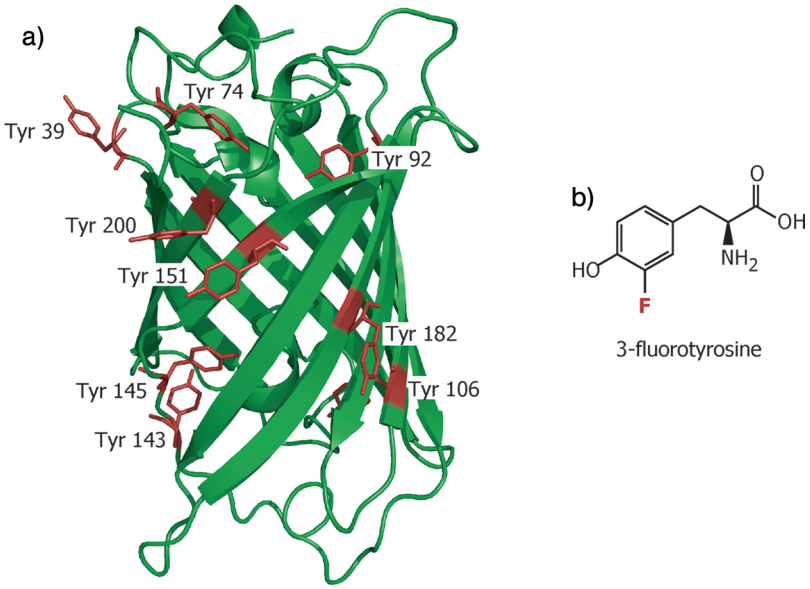

Figure 1.5 Green fluorescent protein (GFP) [11]. (a) The protein fold is depicted in ribbon presentation with the tyrosine residues used for ^{19}F labeling highlighted in red (PDB ID 1B9C). (b) The structural formula of 3-fluorotyrosine.

concentrations of chemical denaturants were qualitatively the same, showing positive enhancement, as all of the fluorotyrosine residues were solvent-accessible in the unfolded state. However, when a low pH value of 2.9 was applied instead, a positive and negative photo-CIDNP effect was found, indicating that folding intermediates with structured parts were still present, and meaning that a low pH is not sufficient to completely denature this protein (Figure 1.5).

Relation of Enzyme Activity to Local/Global Stability of Murine Adenosine Deaminase
Uniformly 6-fluorotryptophan-labeled murine adenosine deaminase (mADA) was expressed in an *E. coli* strain, and by applying ^{19}F NMR spectroscopy, the activity of mADA was examined in the presence of denaturing agents [12]. By adding chemical denaturants, it was observed that mADA lost its enzymatic activity even before significant secondary and tertiary structure transitions had taken place. ^{19}F NMR spectroscopy revealed that the chemical shift change of the ^{19}F resonance of W161 close to the active site exhibited a correlation with the loss of enzymatic activity on the addition of urea. The urea-induced chemical shift change of another fluorinated tryptophan, namely W117, was correlated with the rate constant of the binding event of the transition state analogue inhibitor, deoxycoformycin. The two remaining fluorinated tryptophan residues, W264 and W272, showed hardly any significant chemical shift change upon the addition of small amounts of urea. This indicated that the parts of the mADA protein around the residues W264 and W272 were stable under slightly denaturing conditions. Taken together, the ^{19}F NMR spectroscopic

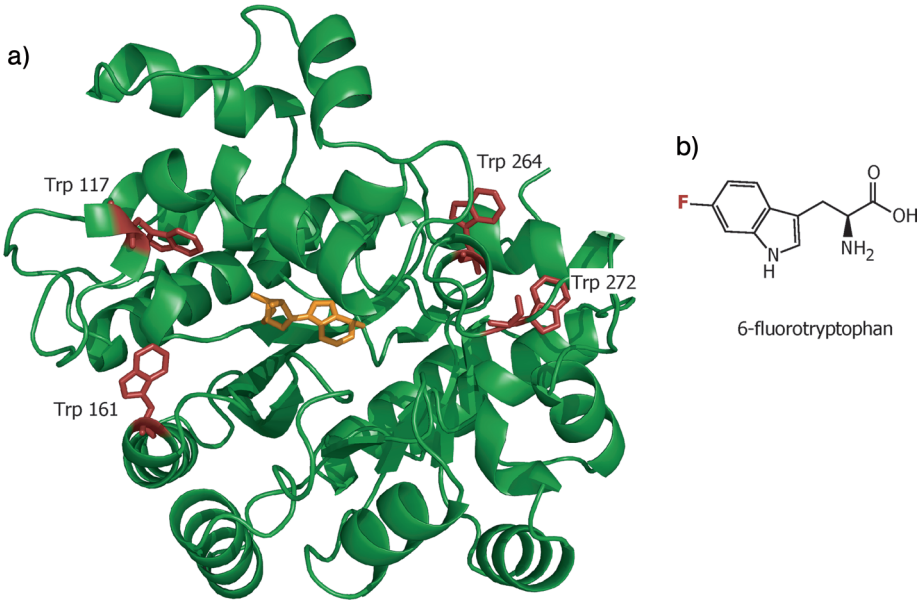

Figure 1.6 Murine adenosine deaminase (mADA) [12]. (a) The protein fold is depicted in ribbon presentation, with the tryptophan residues used for ^{19}F labeling highlighted in red (PDB ID 2ADA); the substrate analogue is highlighted in orange. (b) Structural formula of 6-fluorotryptophan.

results of the fluorinated mADA suggested that different regions of the protein exhibited different local stability upon the addition of urea, which in turn controlled the activity and stability of the protein (Figure 1.6).

Structural Studies of Bcl-xL/Ligand Complexes Fluorine atoms are frequently found in drugs and in drug-like molecules; for example 17% of the compounds listed in the MDDR (MDL drug data report) database contain a fluorine atom. Besides, the introduction of fluorine atoms often improves the pharmacokinetic properties of drug molecules. In a study conducted by Yu and coworkers, fluorinated ligands and the fluorinated protein Bcl-xL were used to derive structural restraints and information of the ligand–protein complex [13]. By using the method derived by Kim *et al.*, a uniformly ^{13}C and para-^{19}F-phenylalanine-labeled protein was expressed in *E. coli* by suppressing the biosynthetic pathway of the aromatic amino acids, phenylalanine, tyrosine and tryptophan, by the addition of the specific inhibitor glyphosphate [6]. Several multidimensional NMR spectra were recorded of the fluorinated Bcl-xL protein alone, and of Bcl-xL in complex with a series of fluorinated ligands (Figure 1.7a; compound **1**: K_D ca. 200 µM; compound **2**: K_D ca. 20 µM). NOEs between ligand **1** and several amino acids of Bcl-xL, A104, L108 and L130, could also be identified. Furthermore, a $^{19}F/^{19}F$ NOESY of the complex of fluorinated ligand **2** and the fluorinated Bcl-xL protein resulted in observable NOE contacts between Phe97 and the fluorine atoms of the ligand (Figure 1.7b) [13]. In conclusion, the

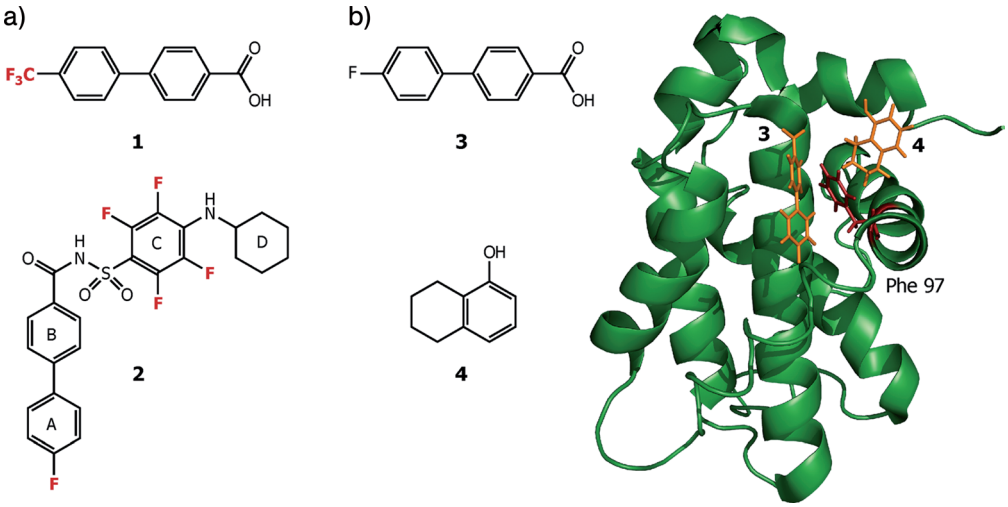

Figure 1.7 The Bcl-xL protein [13, 14]. (a) Typical high-affinity ligands, **1** and **2**. (b) NMR structure of the Bcl-xL protein in complex with 4′-fluoro-1,1′-biphenyl-4-carboxylic acid **3** (orange) and 5,6,7,8-tetrahydronaphthalen-1-ol **4** (orange). The phenylalanine residue 97 at the binding site is highlighted in red (PDB ID 1YSG) [14].

structural data obtained from ^{19}F NMR experiments were in good accordance with the known high-resolution structure of Bcl-xL and highly similar ligands, indicating that fluorine labeling can yield structural information additional to data obtained from traditional ^{13}C- and ^{15}N-labeling. Also in this study, fluorine was proven to be a non-invasive NMR probe nucleus, which did not alter the structural properties of proteins in the first order.

High-Throughput Screening Dalvit and coworkers presented several studies on ^{19}F NMR-based screening techniques for drug discovery [15–22]. NMR-based screening can be used to analyze ligand binding as well as to run functional assays. Thus, by establishing a structure–activity relationship (SAR), the dissociation constants and inhibitory activity of potential binders are accessible. Two ^{19}F NMR-based methodologies were introduced, namely "Fluorine chemical shift Anisotropy and eXchange for Screening" (FAXS) [18, 21] and "Three Fluorine Atoms for Biochemical Screening" (3-FABS) [16, 17].

FAXS is a ligand-based binding competition screening experiment which utilizes a weak affinity spy molecule bearing a CF or CF_3 group. The approach can be further extended by the use of a fluorinated control molecule, which exhibits no affinity against the protein target. These two molecules are selected from existing libraries, which is often an easy task as commercially available libraries contain fluorinated compounds at a rather high frequency (for example, 17% of the compounds listed in the MDL drug data report database). As fluorine atoms increase the lipophilicity of a compound, care must be taken that the "spy" and control substances are still highly soluble in aqueous solution.

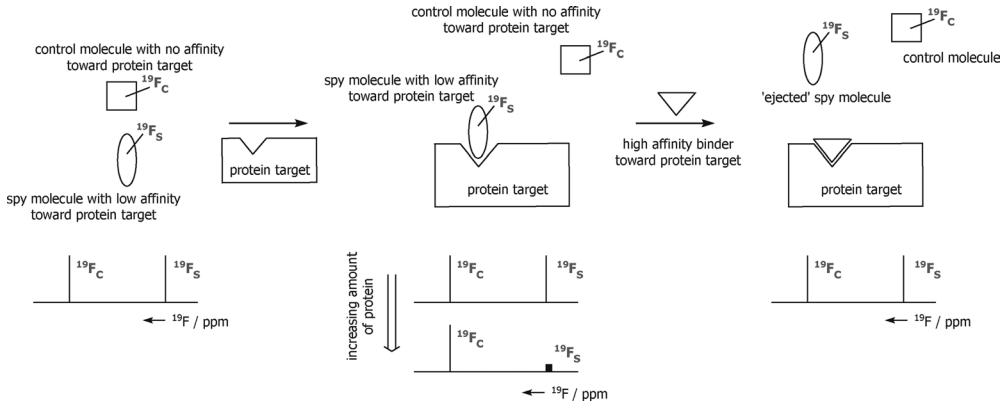

Figure 1.8 Schematics of the "Fluorine chemical shift Anisotropy and eXchange for Screening" (FAXS) approach for high-throughput screening [18, 21].

The spy molecule is replaced by a competing molecule during the screening process of chemical mixtures against the protein target. Thereby, the NMR spectroscopic parameters of the ^{19}F nucleus of the spy molecule are significantly changed (e.g., chemical shift, relaxation parameters). The screening is carried out by monitoring the intensities of the signals of the control and the spy molecule (Figure 1.8). If the K_D value of the spy molecule is known, the binding constants of the competing molecule towards the protein become accessible. It is the large chemical shift anisotropy (CSA) of fluorine that makes the difference in line-width for the spy molecule in the free versus bound state very large, in particular, at high magnetic fields. The FAXS approach, when performed with a weak-affinity fluorinated ligand (spy molecule) and a ^{19}F-labeled control molecule with no affinity toward the target, has proven to be very powerful and sensitive for the primary screening of ligands to a protein target of interest. Furthermore, current technological advances such as ^{19}F cryoprobes strengthen this NMR-based screening approach [15].

The 3-FABS approach (Figure 1.9) is a functional NMR-based assay which is used to study enzymatic reactions and to obtain IC_{50} values (the concentration of inhibitor at which 50% inhibition of the enzymatic reaction is reached) [16, 17]. The functional assay uses CF_3-tags on the enzyme substrates and ^{19}F NMR spectroscopy. Due to modification of the tagged substrate mediated by the enzyme, the chemical environment of the three fluorine atoms is changed, which in turn leads to a chemical shift change. The enzymatic reaction is quenched after a defined delay by the addition of a denaturant, which may be a chelating agent or a strong inhibitor. For screening purposes a reference sample without any test molecules is run, representing 0% inhibition (Figure 1.9a). Even multiple enzymes can be screened by the approach (Figure 1.9b), a point which is of special interest if the selectivity of an inhibitor for a target enzyme is tested in the presence of another enzyme of the same family. Recently, this approach has benefited from current technical advances, such as the introduction of ^{19}F cryoprobes [15].

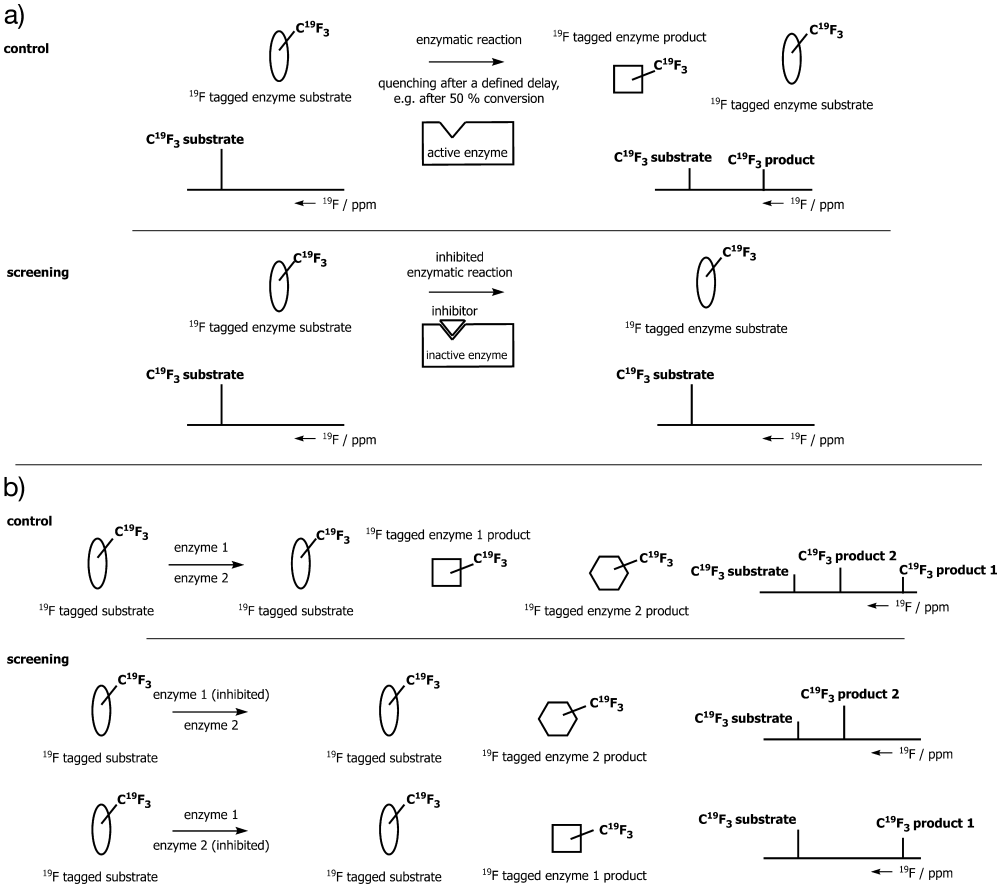

Figure 1.9 Schematic of the "3-*F*luorine *A*toms for *B*iochemical *S*creening" (3-FABS) approach for screening enzyme inhibitors. (a) The principle of 3-FABS screening. (b) Multiple enzyme reactions can be screened using the 3-FABS approach [16, 17].

1.2 ^{19}F NMR Spectroscopy of Nucleic Acids

As described above, ^{19}F NMR spectroscopy not only provides important contributions towards the elucidation of protein structures and dynamics, but also contributes to the field of nucleic acids, where the number of interesting ^{19}F NMR spectroscopic approaches is currently increasing. For nucleic acids, multiple options exists to introduce a fluorine atom, with possible labeling sites being the ribose moieties and the nucleobases. In this respect, the fluorinated nucleoside analogues can be incorporated either by using biochemical methods, or by chemical solid-phase synthesis.

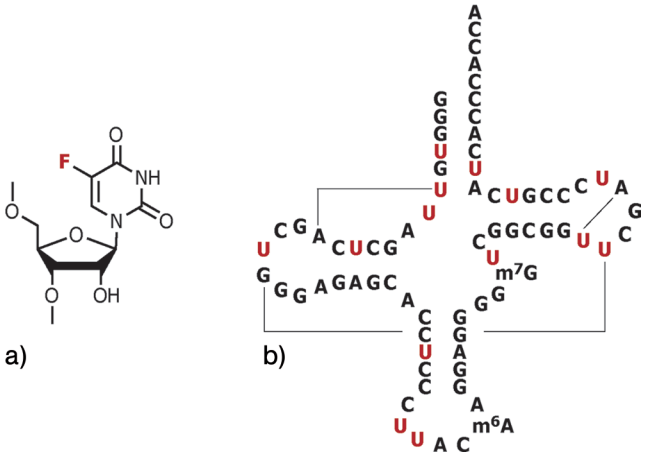

Figure 1.10 *E. coli* $tRNA^{Val}$. (a) Structural formula of a 5-fluorouridine unit. (b) Secondary structure with 5-fluorouridines shown in red. The *in-vitro* transcript lacks the modified nucleobases 7-methyl guanosine (m^7G) and N^6-methyl adenosine (m^6A). The solid lines indicate tertiary structure interactions of the modified uridines [32].

1.2.1 Nucleic Acids with Fluorinated Nucleobases

1.2.1.1 Transfer RNAs

Pioneering studies by Horowitz and coworkers on fluorinated tRNAs were commenced about 30 years ago [23–35]. In these experiments, tRNAs were *in-vitro* transcribed in the presence of 5-fluorouridine triphosphates, such that all uridine positions were replaced by the fluorinated analogue (Figure 1.10). Subsequent NMR spectroscopic characterization led to the assignment of all fluorine resonances. The fluorinated tRNAs were used in multiple studies, including the investigation of the solvent accessibility of a free tRNA and a tRNA in complex with its synthetase [29]. Furthermore, the tRNA constructs were used to assess the interactions with small molecules, such as ethidium bromide or psoralen [23, 25].

1.2.1.2 *HhaI* Methyltransferase in Complex with DNA Duplexes

A fluorinated DNA duplex was used to investigate the nucleotide flipping mechanism during nucleobase methylation mediated by the *HhaI* methyltransferases [36]. The flipping motion was studied by a 5-fluorocytidine placed at the methylation site; a second 5-fluorocytidine residing three nucleotides upstream served as an internal reference (Figure 1.11). The NMR spectroscopic and gel mobility data suggested that, in the binary (DNA/enzyme) and ternary complex (DNA/enzyme/cofactor), the flipping nucleotide (5-fluorocytidine) cycles through three states; namely, the cytidine remains stacked in the double helix, and populates an ensemble of extrahelical conformations and a locked external form in the enzyme active site. The addition of

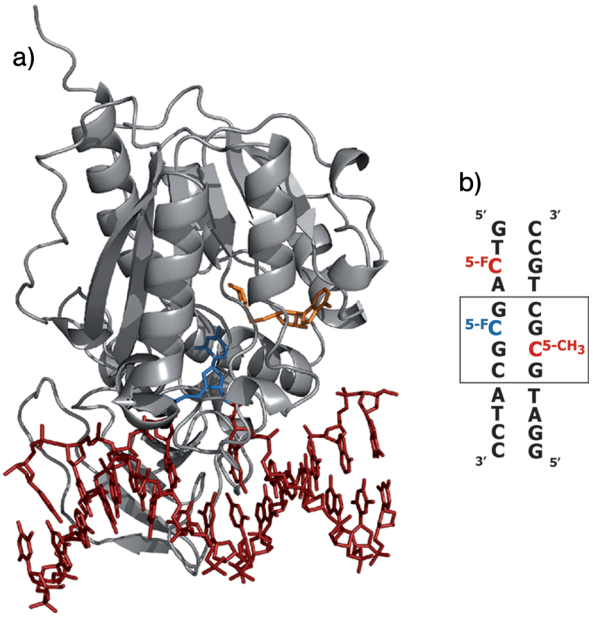

Figure 1.11 *HhaI* methyltransferase. (a) Presentation of the protein in complex with an unmodified DNA duplex (red) and the cofactor analogue AdoHyc (orange). The flipped cytidine residue is highlighted in blue (PDB ID 3MHT). (b) DNA duplex used in the ^{19}F NMR spectroscopic study [36]. The 5-fluorocytidine ($^{5\text{-F}}$C) in red served as internal reference, whereas the $^{5\text{-F}}$C residue in blue represented the target nucleotide for *HhaI* methyltransferase. On the opposite strand, the methyltransferase target nucleotide was replaced by an already methylated cytidine (red).

the cofactor analogue S-adenosyl-L-homocysteine (AdoHyc) led to an enhanced trapping of the target cytidine in the catalytic site of the enzyme. The study showed that the flipping mechanism was not exclusively associated with binding of the cytidine in the active site of the enzyme. Rather, the authors suggested an active role of the methyltransferase in the flipping process, which possibly occurs via the major groove.

1.2.1.3 **Minimal Hammerhead Ribozyme**

The fluorine labeling of nucleic acids has also proven to be very useful in folding studies, as exemplified by monitoring the metal ion-induced folding of the minimal hammerhead ribozyme [37, 38]. Two 2′-*O*-methyl-5-fluorouridines (5-F-U) were incorporated into the hammerhead ribozyme; one (5-F-U4) was located in domain 1, the other (5-F-U7) resided in domain 2, near the interface between the two domains (Figure 1.12) [39].

The fluorine labels responded to folding processes of the hammerhead ribozyme in a very sensitive manner (Figure 1.12). The 5-F-U7 label sensed two events, one of which occurred at a low Mg^{2+} concentration (~0.5 mM). This transition was attributed to the formation of domain 2, which builds the core structure of the

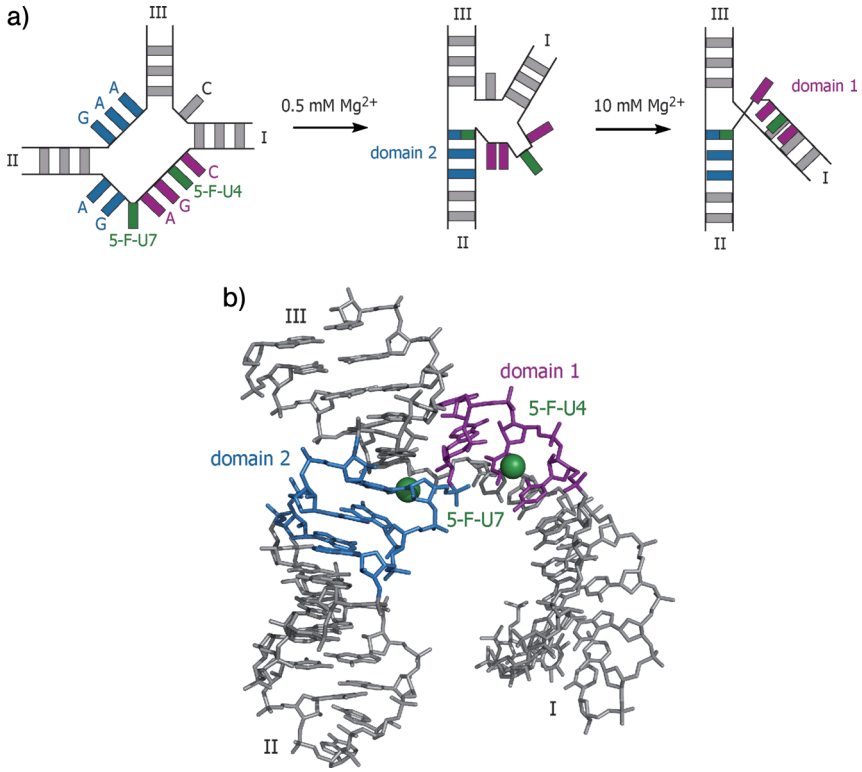

Figure 1.12 The folding process of the hammerhead ribozyme as deduced from ^{19}F NMR spectroscopic data by Lilley and coworkers [39]. (a) The two folding events sensed by the fluorine labels are shown schematically. At low Mg^{2+} concentration (0.5 mM), domain 2 is formed, which is indicated by a chemical shift change and a line width increase of the ^{19}F resonance of 5-F-U7. Above 1 mM Mg^{2+} concentration, domain 1 is formed which is sensed by both fluorine labels. (b) At the time of during the study, the crystal structure of the minimal hammerhead ribozyme (PDB ID 1HMH) [37] was used for structural considerations; the C5 atoms of uridine 4 and 7 are highlighted in green. (Figure adapted from Ref. [39]).

active ribozyme, but it is still not in its functional state (also manifested in the lack of cleaving activity at that magnesium ion concentration). The behavior of the 5-F-U7 label between 0 and 1 mM Mg^{2+} indicated that the fluorine nucleus sensed a reversible exchange process. The broadening of the resonance between 0 and 0.5 mM Mg^{2+} concentration and the subsequent narrowing between 0.5 mM and 1 mM Mg^{2+} probably arose from a fast exchange process between two folding states. By increasing the Mg^{2+} concentration, the exchange rate can be quickened, leading to a narrowing of the ^{19}F resonance at 1 mM Mg^{2+}. By analyzing the line width of the ^{19}F resonance, an approximation of the rate constant k of the exchange process was obtained, resulting in a k of 1000 s^{-1}. At millimolar Mg^{2+} concentrations, both fluorine labels 5-F-U7 and 5-F-U4, sensed the binding of Mg^{2+} which induced a

structural rearrangement of the ribozyme towards the functional state. This second transition was attributed to the formation of domain 1, and followed a two-state model as the ^{19}F chemical shift changes and line width changes of both labels could be fitted to a two-site exchange process. The proposed folding model of the hammerhead ribozyme was later also assessed with fluorescence resonance energy transfer (FRET) studies [40].

1.2.1.4 HIV TAR RNA

^{19}F labeling was also used to study small-molecule binding and to identify the metal ion binding sites of the HIV-1 TAR RNA [41]. Multiple 5-F-U labels were introduced into the target RNA via the phosphoramidite solid-phase synthesis approach (Figure 1.13). In order to test the sensitivity and specificity of the fluorine labels on ligand binding, ^{19}F NMR titration experiments were conducted by adding increasing amounts of argininamide, which is known to bind at the UCU bulge region. The site-specific binding event was reflected via the fluorine labels, as only the resonance of the 5-F-U23 residue was strongly affected during the titration experiment. All other labels responded either moderately (5-F-U25 and 5-F-U38) or only very weakly (5-F-U31 and 5-F-U40) on argininamide binding. This can be easily rationalized by the NMR solution structures of HIV-2 TAR RNA in complex with argininamide [42], and of the ligand-free form of HIV-1 TAR RNA [43]. Whilst U23 is found in a bulged-out conformation for the free RNA, it participates in a base triple formed by U23-A27-U38, in the bound form. This leads to a drastic change in the chemical environment of the ^{19}F resonance of 5-F-U23, and in turn to the observed behavior. By fitting the chemical shift change data of the 5-F-U23 resonance, a dissociation constant for the argininamide ligand could be estimated (K_D ca. 300 μM).

The fluorinated TAR RNA was then probed for metal ion binding sites by titration experiments with Mg^{2+}, Ca^{2+}, and $Co(NH_3)_6^{3+}$. The ^{19}F NMR spectroscopic data showed that metal ions bind preferably at the bulge region and not in the 6-nucleotide loop region. Mg^{2+} and Ca^{2+} ions exhibited a similar affinity towards the bulge region with K_D values in the millimolar range. Co^{3+} ions also showed a site-specific affinity towards the bulge region. Unfortunately, concentrations in excess of five equivalents of $Co(NH_3)_6^{3+}$ led to irreversible aggregation of the RNA, and making determination of the K_D value impossible.

Hennig and coworkers recently reported on an enzymatic method to incorporate fluorinated nucleosides into a target RNA [44, 45]. These authors used 2-fluoroadenosine, 5-fluorocytidine, 5-fluorouridine triphosphates and T7 RNA polymerase for *in-vitro* transcription to obtain uniformly labeled HIV-2 TAR RNAs (Figure 1.14). It was shown that the ^{19}F resonances and imino proton resonances of 2-F-adenosine labeled RNA were easily assignable with a series of homonuclear and heteronuclear NOE experiments (Figure 1.14b) [44]. In a ^{1}H-^{19}F HOESY experiment, intense NOE correlation between the 2-F atoms and the imino protons of two (out of four) 2-F-adenosine residues were found (2-F-A20 and 2-F-A27). Based on a sequential heteronuclear NOE to the anomeric H1′ proton of the 3′ adjacent uridine 23, the ^{19}F resonance of the 2-F-A22 residue was assigned. The remaining ^{19}F resonance of

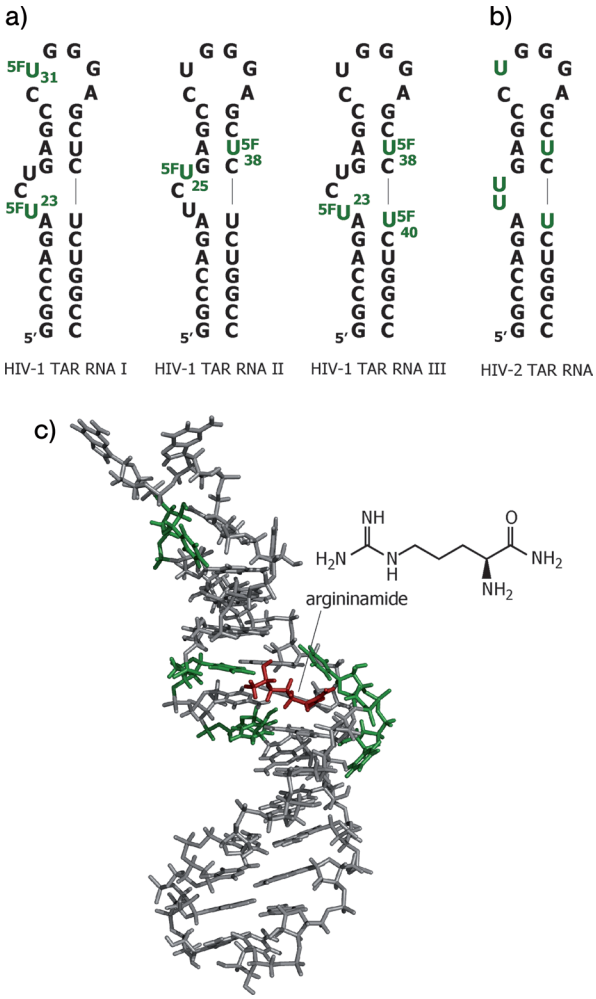

Figure 1.13 HIV TAR RNA. (a) Fluorinated derivatives of HIV-1 TAR RNA (I, II, III) used in the binding study of metals ions (Mg^{2+}, Ca^{2+},$Co(NH_3)_6^{3+}$) and argininamide [41]. (b) Structural formula of argininamide and secondary structure of the HIV-2 TAR RNA with a cytidine deletion in the bulge [42]. (c) NMR solution structure of the HIV-2 TAR RNA/argininamide complex (PDB ID 1AJU) [42]; the uridine residues which were replaced by fluorinated analogues are highlighted in green, the argininamide ligand is highlighted in red.

loop adenosine 35 was assigned by exclusion, as it is the only fluorinated residue in an unstructured RNA domain which exhibits a higher flexibility and no observable heteronuclear NOE correlation.

The study results illustrated that 2-F-adenosine represents a non-invasive NMR labeling nucleus, as the structural integrity of HIV-2 TAR RNA was not impaired and ^{1}H-^{19}F heteronuclear NOEs resembled that of the homonuclear proton NOEs in the unmodified RNA.

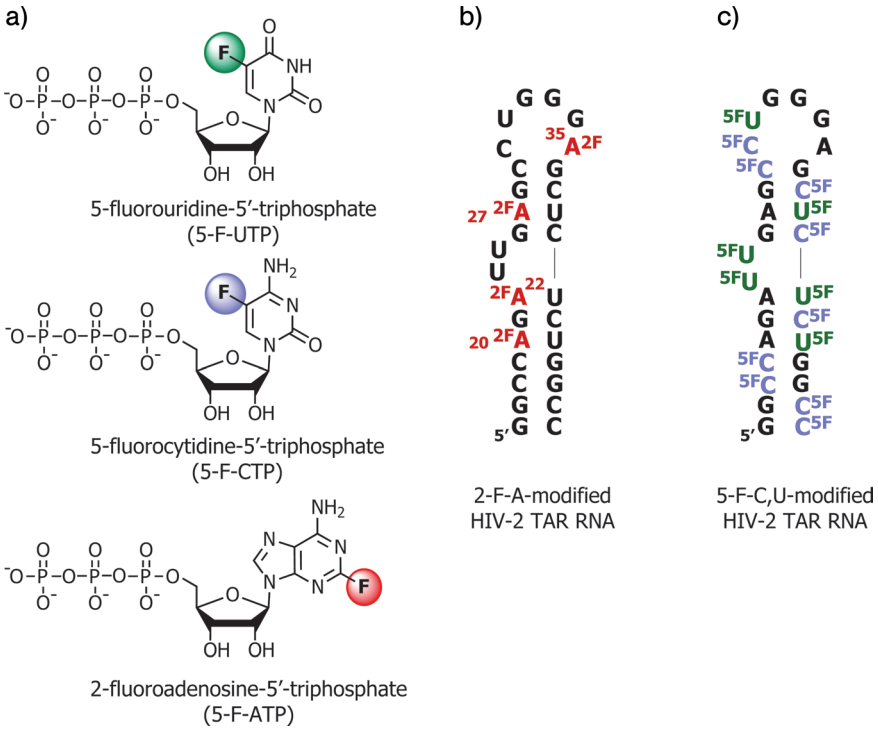

Figure 1.14 HIV TAR RNA. (a) Nucleoside triphosphates for the incorporation of 5-F-uridine (^{5F}U), 5-F-cytidine (^{5F}C), and 2-F-adenosine (^{2F}A) into the RNA targets by *in-vitro* transcription. (b) 2-F-adenosine-labeled HIV-2 TAR RNA [44]. (c) 5-F-pyrimidine-labeled HIV-2 TAR RNA [45].

Furthermore, Hennig and coworkers showed that from a fully 5-fluoropyrimidine-modified RNA, structural information about the nucleobase orientation can be obtained by the analysis of intraresidual ^{5}J(H1′,5F) coupling (Figure 1.14c) [45]. These couplings can also be used to facilitate NMR resonance assignment. The phenomenon of the rather unusual ^{5}J long-range coupling was qualitatively explained by a W-like conformational arrangement of the H1′-C1′-N1-C6-C5-F5 bond network. By applying a density functional theory (DFT) approach, an adequate description of the torsion angle (χ) dependence on the ^{5}J(H1′,5F)-constant was found and described by a generalized Karplus relationship.

1.2.2
Nucleic Acids with Fluorinated Ribose Units

1.2.2.1 *R1inv* RNA

Fewer examples are available of ^{19}F NMR studies on nucleic acids which utilize fluorine-modified riboses. In particular, 2′-deoxy-2′-fluoro (2′-F) nucleosides are

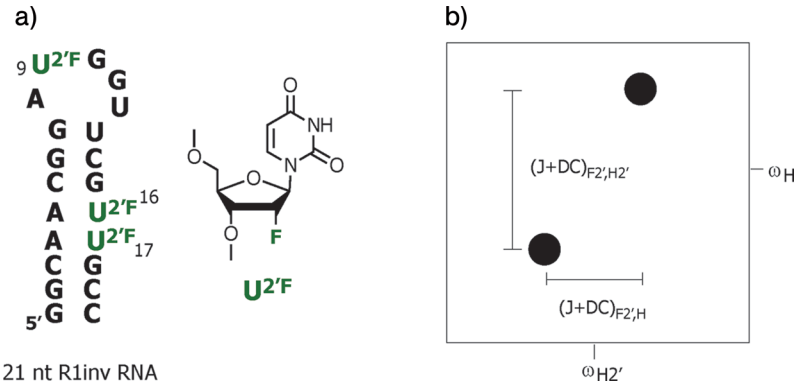

Figure 1.15 *R1inv* RNA. (a) Secondary structure of the 21-nt RNA target hairpin and structural formula of a 2′-F uridine unit [46]. (b) Schematic pattern from a X-filtered E.COSY experiment used for the determination of ^{19}F-^{1}H coupling. The large geminal F2′-H2′ coupling is evolved in the indirect dimension, whereas the long-range F2′-H1′/H3′/H6 couplings are detected in the direct dimension (frequencies ω, dipolar couplings DC).

interesting candidates for non-invasive spin labels, as this modification favors the C3′-endo ribose pucker, which is also the preferred conformation in double-helical A-form RNA. Luy and Marino introduced 2′-F-modified uridine residues at positions 9, 16, and 17 of the *R1inv* RNA hairpin (Figure 1.15a) [46]. The RNA was partially aligned by using filamentous bacteriophage Pf1 [47] and, by applying X-filtered-E.COSY-type methods, long-range dipolar coupling constants between $^{19}F/^{1}H$ spin pairs were obtained. In the experiment, the X-filter was tuned on a scalar coupling constant of approximately 50 Hz, selecting the ^{2}J(H2′,F2′) coupling constant. After the X-filter and evolution in t1 of the H2′ protons' chemical shifts and scalar couplings, the H2′ magnetization was correlated via a homonuclear mixing step to other protons. Finally, the long-range correlated protons (H3′, H1′ and H6 base protons) were detected without ^{19}F decoupling (Figure 1.15b).

The $^{19}F/^{1}H$-dipolar couplings were used in structure determination and refinement of the hairpin RNA. The obtained dipolar couplings of the fluorinated uridine residues placed in the double helix (positions 16 and 17) were in perfect agreement with a modeled UUG trinucleotide in A-form geometry. The authors further suggested that selective fluorine labeling of RNAs and the subsequent residual dipolar coupling (RDC) analysis might be a valuable tool in determining the interhelical orientations of large RNAs or RNA–protein complexes. However, care must be taken, if 2′-fluorinated nucleotide analogues are placed in non-canonical regions, where deviations of the standard A-form geometry are possible. In this study, the 2′-fluororuridine at position 9 was found to have a shifted C2′/C3′-endo population (towards C3′-endo), as compared to the C2′-/C3′-endo equilibrium position of uridine 9 found in the unmodified hairpin. To summarize, the selective labeling of double-helical RNA regions with fluorinated nucleotide analogues should